ACS APPLIED MATERIALS & INTERFACES

Research Article

www.acsami.org

"Evaporating" Graphene Oxide Sheets (GOSs) for Rolled up GOSs and Its Applications in Proton Exchange Membrane Fuel Cell

Kai Feng, Beibei Tang,* and Peiyi Wu*

State Key Laboratory of Molecular Engineering of Polymer and Department of Macromolecular Science and Laboratory of Advanced Materials, Fudan University, Shanghai 200433, People's Republic of China

Supporting Information

ABSTRACT: In the present work, we prepare rolled up graphene oxide sheets (GOSs) by "evaporating" GOSs from their dispersion to a remote aluminum foil surface. The topological structure of the rolled up GOSs on the aluminum foil surface, which is determined by the quantity of the formed Al^{3+} ions from the reaction between the alumina on the aluminum foil surface and the weak acidic condensed vapor of the GOS dispersion, can be easily controlled via simply changing the H_2O content in the original GOS dispersion. Meanwhile, a GO/Nafion composite membrane for proton exchange membrane fuel cell is successfully prepared utilizing the as-obtained hole-like self-assembled structure of the rolled-up GOSs as a supporting material. The resultant composite membrane exhibits excellent proton conductivity compared to that of the recast Nafion membrane, especially under low-humidity conditions. An increase in proton conductivity by several times could be easily observed here, which is mainly attributed to the rearrangement of the microstructures of Nafion matrix to significantly facilitate the proton transport with rolled up GOSs being independently incorporated. The method reported here offers new degrees of freedom to achieve such transformations among the allotropic forms of carbon and/or develop new carbon material/polymer composite materials with excellent properties.

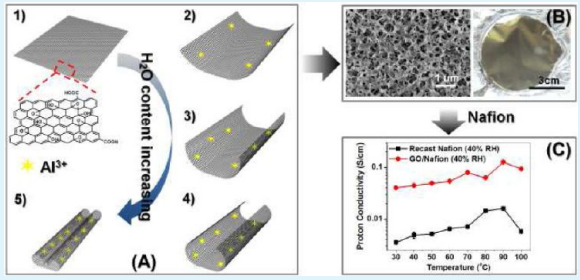

KEYWORDS: *graphene oxide, evaporation, carbon nanoscroll, topological transformation, porous supporting material, Nafion, proton exchange membrane*

1. INTRODUCTION

Carbon, appearing in such diverse allotropic forms as zero-dimensional (0D) buckyballs, 1D nanutubes (CNTs), 2D graphene, 3D graphite or diamonds, etc., is the research hot spot in the current material science and engineering.[1,2] Its distinctive electrical, optical, mechanical, and thermal properties have been enormously investigated for potential applications in many areas, especially after the rise of graphene.[1] Besides the transformation among these allotropic forms, such as unzipping CNTs to graphene nanoribbons,[3,4] converting graphene oxide to fullerenes,[5] rolling up graphene into multiwalled carbon nanotubes (MWNTs),[2] and graphene oxide sheets (GOSs) into carbon nanoscrolls (CNSs),[6,7] it has also attracted considerable research interests from where some novel materials with enhanced properties hence stem.[4,7,8] These topological transformations are particularly necessary and important in preparing carbon material/(in)organic material hybrids (such as carbon material/polymer composites) which may bring a bright future for multidisciplinary technologies,[7] dye -sensitized solar cells,[9] photocatalysts,[10,11] biosensors,[12,13] and drug carriers,[14,15] for example. Noteworthily, among the existing researches, the sonication effect[2,5,7,8,16] is vastly employed to achieve such transformations while few other effective approaches have hitherto been developed, which certainly sets a limit to the further exploration of new carbon material and its composites. Meanwhile, despite the advantages of simple operation, high yield, and low energy consumption of the sonication chemistry,[7] the sonication effect may break the basic structure of such carbon materials or even fracture them completely and hence damage the resultant composite materials,[5,17] leading to an urgent need to find a more gentle method.

Our previous work found that GOSs could transfer from their evaporating aqueous dispersion to the remote aluminum foil (see Figure S1 in the Supporting Information) because of the strong hydrogen bonding interactions between GOSs and the water vapor molecules and spontaneously transform into rolled up GOSs with the aid of Al^{3+} ions.[6] The GOSs aqueous dispersion provides an acidic condensed water vapor due to the existence of GOSs, promoting the transformation from alumina on the aluminum foil surface to Al^{3+} ions.[6,18] Actually, such a transformation from which a GOS-multivalent metal ions hybrid (to put it more precisely: a CNS−multivalent metal ion hybrid) results is fairly difficult to be achieved via conventional approaches, because a GO hydrogel would appear upon directly adding some multivalent metal ions into the GOSs aqueous

Received: December 6, 2012
Accepted: January 21, 2013
Published: January 21, 2013

dispersion,[19] let alone the transformation from GOSs into CNSs. Each multivalent metal ion interacting with multiple GOSs is probably the main reason for the GOSs gelation. As a matter of fact, to date, only those additives that cannot induce the GOSs gelation are applied to realize the transformations, such as Ag and Fe_3O_4 nanoparticles,[7] nitric acid,[5] etc. The obstacle in achieving the transformation from GOSs into CNSs by multivalent metal ions could be skilfully avoided through the GOSs' "evaporation" where GOSs probably transfer from their dispersion to the surface of certain remote metal material independently.[6]

Furthermore, we believe that such an independent-transfer phenomenon of GOSs has great potential applications in preparing GO/polymer composite materials. Take the holelike self-assembled structure of the rolled up GOSs on the aluminum foil surface for instance, the GO layer could act as an excellent supporting material onto which certain polymer solution could be carefully casted to completely fulfill the space among those independent GOSs. Compared to those GO/polymer composite materials prepared by simply adding GOSs or (polymer-) functionalized GOSs into the polymer solution and then sonicating the resultant mixture to help GOSs disperse inside the polymer matrix, the composite materials obtained here probably have much more outstanding properties because of the extremely good dispersion of GOSs inside the polymer (i.e., probably disperse independently) and hence better interactions of GOSs and the polymer matrix. To verify this proposal, accordingly, we tentatively prepare a GO/Nafion composite membrane for proton exchange membrane fuel cell by casting Nafion solution on the holelike self-assembled GO layer and then dissolving the aluminum foil with dilute HCl after the formation of the Nafion membrane on the layer. GO could interact with both the nonpolar backbone domains and the polar ionic cluster domains of Nafion matrix because of its amphiphilic nature, which could reorganize the proton transport channels to benefit the improvement of the membrane conductivity.[20,21] Moreover, as aforementioned, the independent dispersion of each GOSs inside the Nafion matrix probably could significantly enhance the improvement of proton conductivity, even under harsh conditions such as high operation temperature and/or low humidity.

Therefore, the evaporation phenomenon of GOSs has a favorable application foreground in both the transformation of those aforementioned allotropic forms of carbon and the preparation of novel GO/polymer composite materials. In this contribution, based on the already-obtained knowledge that the quantity of multivalent metal ions (take the Al^{3+} ions for instance) may be crucial to the topological structure of the "evaporated" GOSs on the aluminum foil surface, we rationally further extend this novel technology and accordingly propose a facile approach to prepare rolled up GOSs with different topological structures successfully via controlling the H_2O content in the original GO dispersion and hence the quantity of the formed Al^{3+} ions. Besides, the resultant GO layer on the aluminum foil surface was utilized to prepare the GO/Nafion composite membrane. Our experimental results demonstrate that the GO/Nafion composite membrane obtained by our method exhibits much better performance compared to the recast Nafion membrane. The proton conductivity of our GO/Nafion composite membrane improves prominently due to the well dispersion of GOSs inside the Nafion matrix, especially under low operation humidity (an improvement of proton conductivity by several times could be easily observed here), rendering our method as a very promising approach to prepare high-performance GO/polymer composite materials by "evaporating" GOSs.

2. EXPERIMENTAL SECTION

2.1. Materials. Expandable graphite powders were provided by Yingtai Co. (China). Nafion solution (perfluorinated resin solution, 5 wt % in lower aliphatic alcohol and water mixture) is obtained from DuPont. Unless otherwise stated, all the other reagents were purchased from commercial suppliers and were used as received.

2.2. Self-Assembly of Rolled up GOSs on the Remote Aluminum Foil Surface under Different Evaporation Conditions. *2.2.1. Preparation of GOSs.* GOSs were produced from graphite power by a modified Hummers method, the same as that in our previous report.[6] 15 g of expandable graphite powders and 115 mL of concentrated H_2SO_4 were mixed and agitated in an ice bath. Then, 15 g of potassium permanganate was added to the suspension slowly to prevent a rapid rise in temperature (less than 20 °C). After being kept in the ice bath for 2 h, the reaction mixture was heated to 35 °C and then stirred continuously for 30 min; 115 mL distilled water was slowly added into the reaction vessel. The diluted suspension was stirred for another 15 min and further diluted with 700 mL of warm distilled water (40 °C) followed by adding 50 mL of 30% H_2O_2. The resulting suspension was then filtered, washed with 5% HCl and dialyzed for 7 days in the dark. Subsequently, the wet form of graphite oxide was freeze-dried, pulverized and finally vacuum-dried at 60 °C for 24 h.

2.2.2. Synthesis of Rolled up GOSs with Different Topological Structures. 10 mg of GOSs were dissolved in 100 mL of mixed solvent (H_2O/THF, or H_2O/NMP, or H_2O/DMF; and the H_2O content varies from 0 v/v% to 80 v/v% of the mixed solvent) in a glass beaker (150 mL). Then the mixture was agitated for 30 min at room temperature to obtain a stable GO dispersion. The glass beaker containing the resulting GO dispersion (0.1 mg/mL) was covered by an aluminum foil (see Figure S1 in the Supporting Information) plainly and then sealed with preservative film carefully. The whole system was then placed in an oven at desired evaporation temperature for 48 h. At last, the aluminum foil on which the "evaporated" GOSs deposited was dried gradually at room temperature. The resultant CNSs with different topological structures were obtained by dissolving the "CNSs/aluminum foil" with HCl followed by dialyzing for 7 days.

2.2.3. Characterizations of Rolled up GOSs. The morphologies of the self-assembled structure of GOSs on the remote aluminum foil surfaces were observed with a scanning electron microscopy (SEM, XL 30 ESEM-TMP PHILIP) and/or a field emission scanning electron microscopy (FE-SEM, Hitachi, S-4800). All samples were coated with gold before (FE-)SEM observation. Atomic force microscopic (AFM) images were obtained using a Multimode Nano 4 in the tapping mode. Transmission electron microscopy (TEM) images and energy dispersive spectrometer (EDS) analyses were recorded on a JEOL JEM2100 TEM instrument operated under an acceleration voltage of 200 keV. The CNSs on aluminum foil surface (see Figure S1 in the Supporting Information) prepared at 50/80 v/v% H_2O (THF) under 45 °C for 48 h were obtained by dissolving the aluminum foil with HCl and then dialyzing the resulting acidic aqueous solution for 7 days before AFM, TEM, and EDS measurements. Thermogravimetric analysis (TGA) measurements of the aluminum foil on which GOSs had deposited were performed under N_2 atmosphere with a Perkin-Elmer Thermal Analyzer at a heating rate of 20 °C/min.

2.3. GO/Nafion Composite Membrane. *2.3.1. Preparation of the GO/Nafion Composite Membrane.* About half of the solvent of the as-received Nafion solution was removed by rotary evaporation under 50 °C and then DMF was added into the resultant concentrated Nafion solution followed by rotary evaporating for another 10 min at 60 °C. The obtained Nafion solution was carefully casted on the surface of the hole-like self-assembled GO layer with the aid of a rectangular model in an amount that would give the membrane with a thickness of about 50 um. The model was first placed horizontally under a little negative-pressure condition for several minutes to

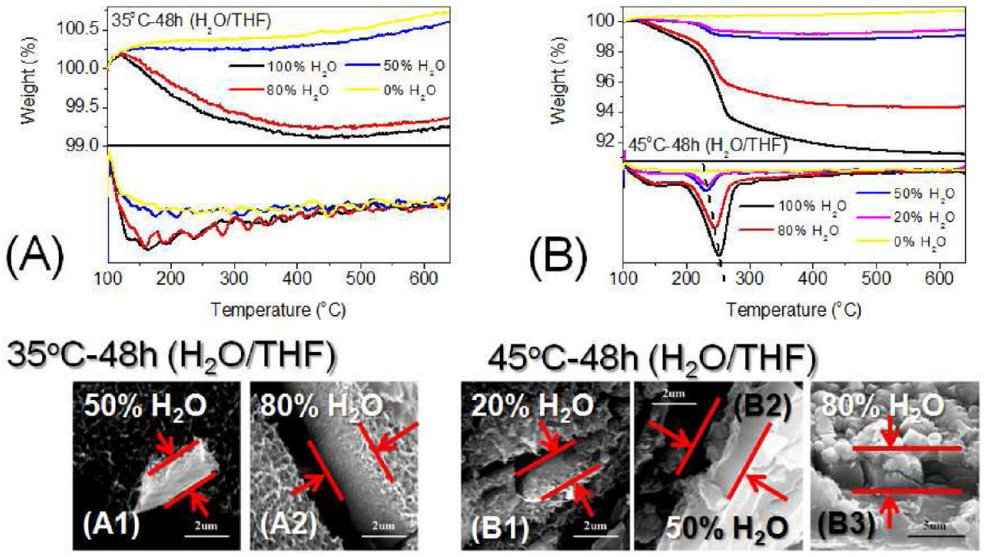

Figure 1. (A, B) TG analyses of the sample "GO/aluminum foil" obtained at different H_2O contents (H_2O/THF) under 35/45 °C for 48 h, respectively (N_2, 20 °C/min). (A1, A2, B1−B3) Corresponding sectional SEM images of the GO (CNS) deposit layers on the aluminum foil surface (see Figure S1 in the Supporting Information) at different H_2O contents under 35/45 °C for 48 h.

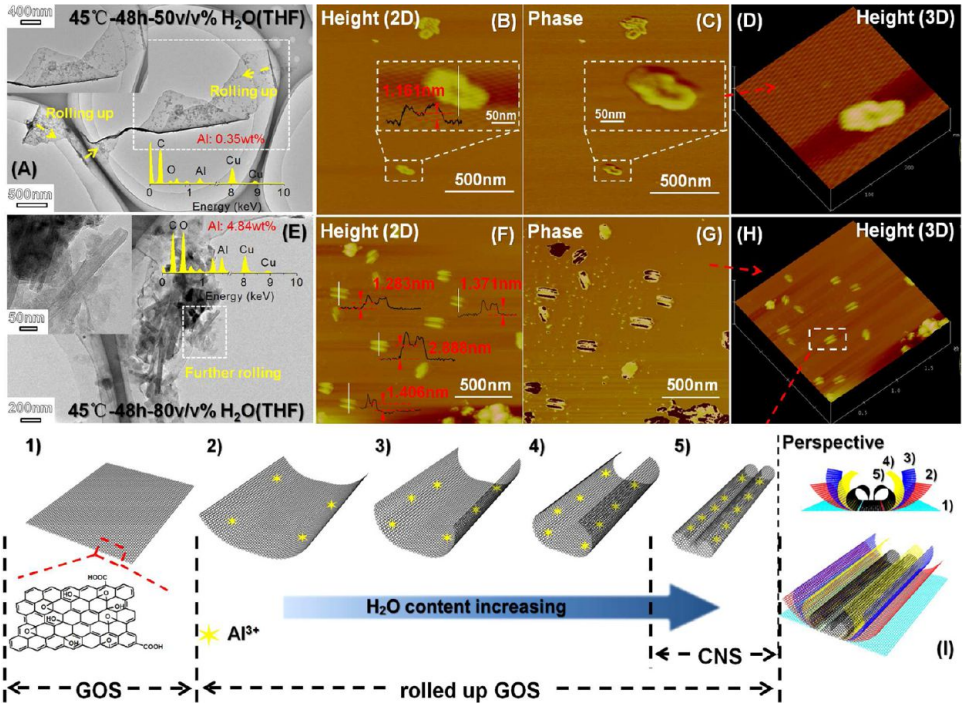

Figure 2. (A−H) TEM, EDS, and AFM characterizations of the rolled up GOSs prepared at 50/80 v/v% H_2O under 45 °C for 48 h (H_2O/THF); (I) schematic quantity (of Al^{3+} ions)-dependent rolling process of the "evaporated" GOSs on the aluminum foil surface (see Figure S1 in the Supporting Information).

facilitate the diffusion of polymer into the place among the "evaporated" GOSs. Second, the model was dried in a vacuum oven by slowly increasing the temperature from 70 to 120 °C for 6h, and then further dried under vacuum at 120 °C overnight. Third, the aluminum foil was carefully dissolved with dilute HCl to obtain a "free-standing" GO/Nafion composite membrane. At last, the composite membrane was boiled in 3 wt % H_2O_2 solution at 70 °C for 2h, followed by the immersion in 1 M H_2SO_4 solution for 1h at 80 °C to convert the membrane into H^+ form. The prepared GO/Nafion composite membrane was rinsed by deionized water several times before latter characterizations. The recast Nafion membrane was prepared via the same approach described above.

2.3.2. Characterizations of the Recast Nafion Membrane and the GO/Nafion Composite Membrane. The cross-sectional morphologies of these proton exchange membranes were observed with a SEM (XL 30 ESEM-TMP PHILIP). The samples were coated with gold before SEM observation. The AFM images were obtained using a Multimode Nano 4 in the tapping mode. X-ray diffraction (XRD, PANalytical X'pert diffractometer with Cu Kα radiation) was utilized to characterize the influence of GOSs on the microstructures of the composite membrane. The FT-IR spectra of membranes were measured on a Nicolet Nexus 470 spectrometer with a resolution of 4 cm^{-1} and 64 scans. The proton conductivities of membranes were obtained by a four-electrode method using AC impedance spectros-

dx.doi.org/10.1021/am302995c | ACS Appl. Mater. Interfaces 2013, 5, 1481−1488

copy between 0.1 MHz and 1 Hz with potentiostat control (CHI660d model). The investigated temperature and humidity were controlled by a temperature-and-humidity test chamber. All the samples were placed under the desired temperature and humidity for 8h before the measurements of proton conductivity. The water uptake (WU) was obtained to characterize the water retention capability of each membrane. The membranes were first dried at 80 °C for 24 h and then weighed (W_{dry}). Second, they were immersed in deionized water at room temperature for 24 h to be saturated. Then they were taken out followed by removing the water quickly away from the membrane surface before weighing (W_{wet}). The WU could be calculated by the following equation:

$$\mathrm{WU}(\%) = \frac{W_{wet} - W_{dry}}{W_{dry}} * 100$$

3. RESULTS AND DISCUSSION

3.1. Rolled up GOSs with Different Topological Structures. In the present work, the system of 0.1 mg/mL GOSs/mixed solvent (a mixed solvent of H_2O and THF; and the H_2O content varies from 0 v/v% to 80 v/v%) under various evaporation conditions (35/40/45/55 °C for 48 h) is carefully investigated. No typical experimental results have been found that GOSs could transfer from their evaporating organic (THF, or NMP, or DMF) dispersions. Pellucidly, a higher H_2O content in the original GOSs dispersion promotes the occurrence of a larger amount of water vapor molecules and "evaporated" GOSs and hence more formed Al^{3+} ions from the reaction of the acidic condensed vapor and the alumina on the aluminum foil surface, with other evaporation conditions determined. Under this circumstance, more GOSs could deposit on the aluminum foil surface by the aid of the strong coordinate bonds between their epoxy or hydroxyl groups and these Al^{3+} ions, as the H_2O-content-dependent thickening process of the GO deposit layer demonstrated in the sectional SEM images (Figures 1A1, A2, B1−B3, and Figures S2/3 in the Supporting Information) and the weight loss of the sample "GO/aluminum foil" at 600 °C shown by the TGA analyses (Figure 1A, B).

GO would yield CO, CO_2, and steam at certain temperature because of the pyrolysis of their labile oxygen-containing functional groups, corresponding to the mass loss around 230 °C in the TGA analyses.[22] Obviously in panels A and B in Figure 1, this pyrolysis temperature of GOSs increases with the H_2O content in the original GOSs dispersion. It confirms that more oxygen-containing functional groups of an individual GOS could interact with Al^{3+} ions and hence were stabilized (i.e., the interaction between an individual GOS and Al^{3+} ions is stronger) at higher H_2O content. This phenomenon parallels the discovery in the energy dispersive spectrometer (EDS) analyses (of the parts indicated by the white boxes in panels A and E in Figure 2 that a higher percentage of Al is trapped in the rolled up GOSs at higher H_2O content. The quantity of the trapped Al in rolled up GOSs could reach 7.18 wt % at 100 v/v % H_2O under 45 °C for 48 h.[6] It indicates that we could easily control the quantity of the formed Al^{3+} ions interacting with the "evaporated" GOSs on the remote metal surface through simply changing the H_2O content in the original GOSs dispersion. Moreover, both the differences of the quantity and the pyrolysis temperature of GOSs at different H_2O contents appear more evident at higher evaporation temperature, as presented in Figure 1B1−B3 and B, respectively. All these conclusions can be obtained from the system of 0.1 mg/mL GOSs/mixed solvent (a mixed solvent of H_2O and NMP or DMF; and the H_2O content varies from 0 v/v% to 80 v/v% of the mixed solvent), similarly (see Figure S4 in the Supporting Information). Noteworthily, according to the TG curve of the fresh aluminum foil (see Figure S5 in the Supporting Information), we suppose that a very tiny amount of AlN formed from the side-reaction $2Al + N_2 \rightarrow 2AlN$ during the heating process probably leads to the slightly increase of the sample weight at the late stage of the TGA characterization. This phenomenon is especially obvious at 35 °C, where the amount of the deposited GOSs on the aluminum foil surface is relatively small (Figure 1A), making the TG curves now very different from that of commercial GO.

We obtained the rolled up GOSs through dissolving the "GO/aluminum foil" by HCl followed by dialyzing for 7 days before the TEM, EDS, and AFM measurements (take the 0.1 mg/mL GO/solvent (50 v/v% H_2O (THF) and 80 v/v% H_2O (THF)) at 45 °C for instance, Figure 2A−H). As we had anticipated, the quantity of Al^{3+} ions is crucial to the topological structure of the "evaporated" GOSs on the aluminum foil surface. More Al^{3+} ions would further enhance the rolling process of GOSs via forming more coordinate bonds with the epoxy or hydroxyl groups of GOSs, promoting the transformation from the original 2D structure gradually into 3D nanoscrolls, as schematically illustrated in Figure 2I and experimentally proved by Figure 2A−H (including Figures S6/7 in the Supporting Information). It gives us a great opportunity to obtain rolled up GOSs with different topological structures. Besides, it is worth noting that the residual oxygen-containing functional groups of the "evaporated" GOSs prefer to interact with the protons rather than the Al^{3+} ions formed during the HCl-resolving process because of the overwhelmingly high concentration of the H^+ ions. Meanwhile, during the HCl-resolving process, the coexistence of a large amount of multivalent metal ions and GOSs would lead to great probability of one Al^{3+} ion generally interacting with multiple GOSs and hence the formation of GO hydrogel, rather than promoting the rolling up of individual GOS.[19] In a word, we believe that the HCl-resolving process has little influence on both individual GOS's rolling up and its Al contents.

This rolling process of GOS could be simply depicted as follows (Figure 2I): GOSs "evaporate" from their dispersion and then deposit on the aluminum foil surface accompanied by the formation of Al^{3+} ions from the reaction of the acidic condensed vapor and the alumina.[6] These Al^{3+} ions would first localize themselves at the edges of a GOS (indicated by the yellow arrows in Figure 2A and Figure S6 in theSupporting Information) and then template the initial rolling up of the GOS (Figures 2A−D and G-2, Figure S6 in the Supporting Information) via forming coordinate bonds with multiple oxygen-containing functional groups of the GOS. With the H_2O content increasing, more Al^{3+} ions would subsequently arrive at the very site to drive the further rolling process of the GOS where they remain trapped (Figure 2E−H and G-5, Figure S7 in the Supporting Information).

Under the same evaporation conditions, the GOS would transform into a CNS completely when the H_2O content is 100 v/v% in the original GOSs dispersion.[6] This mechanism reflects the quantity (of multivalent metal ions)-dependent-rolling principle of GOSs, which provides a cogent basis to guide the preparation of rolled up GOSs with different topological structures.

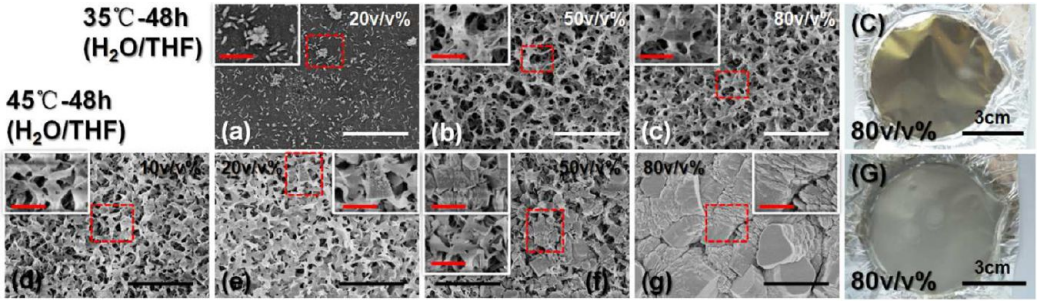

Figure 3. (a–g) FE-SEM images of the GO deposit layer on the aluminum foil surface (see Figure S1 in the Supporting Information) at different H_2O contents under 35/45 °C for 48 h, respectively (bar = 2 um). The morphology of the parts indicated by the red boxes can be obtained from the insets at a higher resolution with bar = 500 nm. (C, G) Corresponding digital photos at 80 v/v% H_2O under 35/45 °C for 48 h, respectively.

As demonstrated in our previous work where the H_2O content in the original GOSs dispersion is 100 v/v%, the rolled up GOSs would first form holelike structures, and then congregate to form cell-like aggregates, and then conelike aggregates (stacked by the cell-like aggregates), and finally cylindrical-like aggregates (by the accumulation of the conelike aggregates) on the aluminum foil surface.[6] Furthermore, the self-assembly behavior of these rolled up GOSs presents an evaporation-time (and/or temperature)-dependent character.[6] In the current study, at first glance, it seems that the self-assembled structure of the rolled up GOSs would similarly evolve from the hole-like structure to the cylindrical-like structure as the H_2O content increases in the original GOSs dispersion (i.e., H_2O-content-dependent self-assembly), as shown in Figure 3 (including Figures S8–S29 in the Supporting Information). However, the typical lamellar structure of GOSs can be observed at low H_2O content in the FE-SEM images (for example, Figure 3d, e and Figure S21/S22 in the Supporting Information, etc.), which coincides well with the H_2O-content-dependent rolling process of GOSs on the aluminum foil surface. Low H_2O content in the original GOSs dispersion could not provide enough Al^{3+} ions for the transformation of the "evaporated" GOSs into CNSs. That is why the well-constructed cell-like aggregates cannot be formed under low H_2O content (Figures S16/S17/S20 in the Supporting Information, etc.). Although we observe variability for these (FE-)SEM studies, the overall trend of the self-assembled structure evolution of GOSs with the H_2O content was consistent throughout. We provide as many (FE-) SEM and AFM images of these self-assembled structures as we can in the ESI to prove this phenomenon (see Figure S9–S29 in the Supporting Information). Similarly, all these discoveries can be confirmed by the system of 0.1 mg/mL GOSs/mixed solvent (a mixed solvent of H_2O and NMP or DMF), as the (FE-)SEM images shown in Figures S30–S49 in the Supporting Information.

3.2. GO/Nafion Composite Membrane. The mutual interactions between Nafion matrix and GOSs could rearrange the microstructures of the backbone domains and the ionic cluster domains of Nafion, which would significantly enhance the performance of the composite membranes, such as thermal (stabilizing the backbones and side chains of Nafion), mechanical (increasing the membrane's tensile strength and Young's modulus) and electrical properties (improving membrane's proton conductivity).[20,21] Compared to the cylindrical-like self-assembled structure, the holelike one is more suitable to prepare GO/Nafion composite membranes. Because the polymer chains could diffuse and then fulfill the abundant holes of the holelike structure during the casting process, which undoubtly benefits the incorporation of GOSs into the Nafion matrix and hence the improvement of the performance of the resultant membranes. Therefore, we select the sample "35 °C-20 v/v%THF" (Figure 3c) as the supporting subject investigated.

As shown in A and B in Figure 4, the GO/Nafion composite membrane is colorless and transparent, almost the same as the

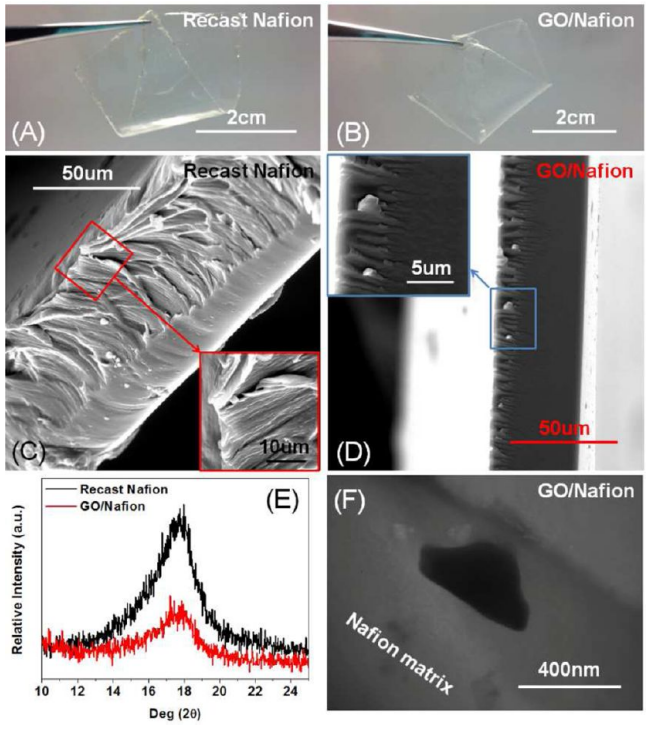

Figure 4. (A/B, C/D) Digital photos and cross-sectional SEM images of the recast Nafion membrane and the GO/Nafion composite membrane, respectively; insets in C/Dare the morphologies of the parts indicated by boxes at a higher resolution; (E) XRD patterns of the two membranes; (F) cross-sectional TEM images of the GO/Nafion composite membrane.

recast Nafion membrane, which indicates that very low amount of GOSs are incorporated into the membrane matrix. This phenomenon is easily to be understood based on the fact that only a small quantity of GOSs could "evaporate" and then deposit on the aluminum foil surface. Besides, not all these deposited GOSs could be incorporated into the Nafion matrix because the holes stemmed from the self-assembly of GOSs

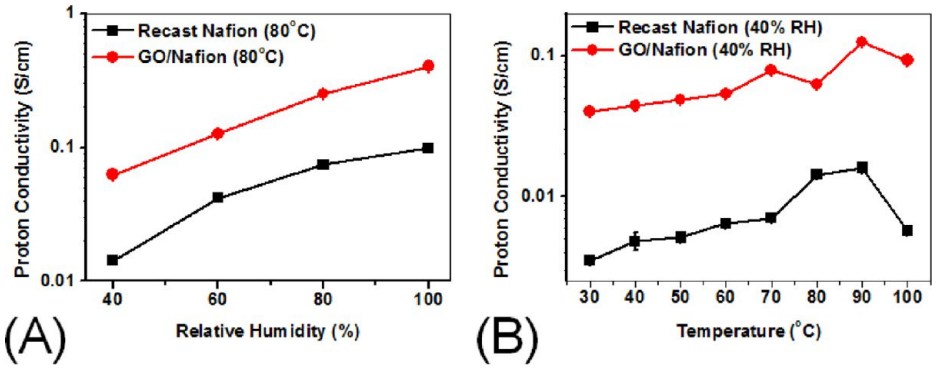

Figure 5. (A) Humidity-dependent proton conductivity plots (80 °C) and (B) temperature-dependent proton conductivity plots (40% RH) of the recast Nafion membrane and the GO/Nafion composite membrane.

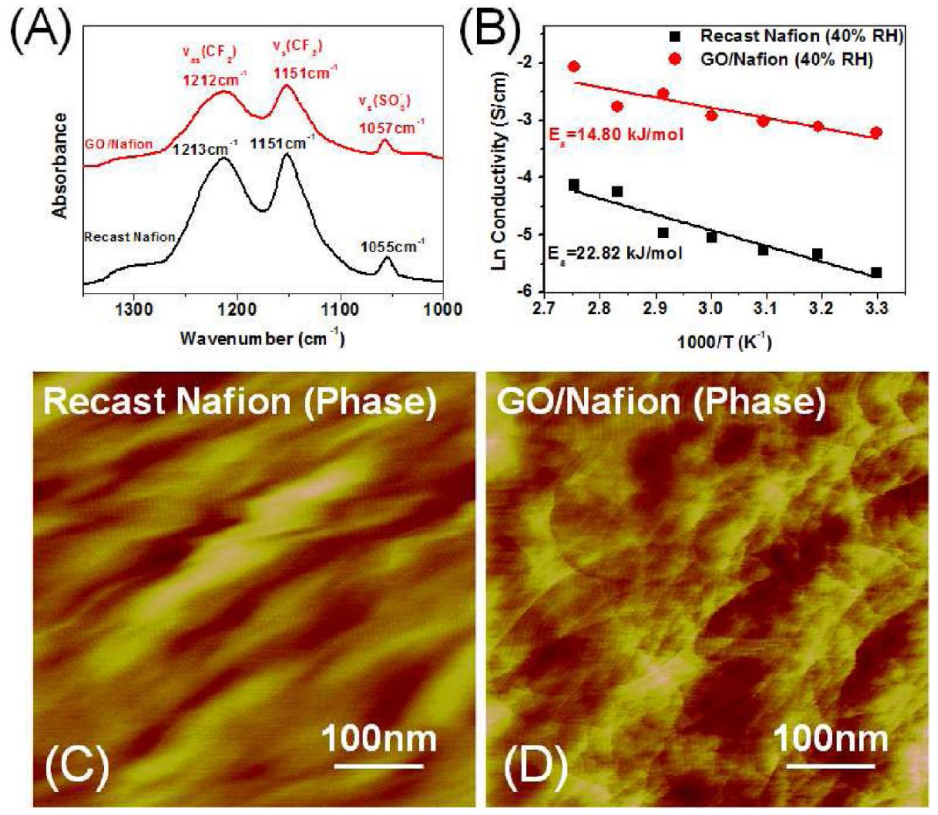

Figure 6. (A, B) FT-IR spectra and Arrhenius plot of the recast Nafion membrane and GO/Nafion composite membrane, respectively; (C/D) AFM phase images of the recast Nafion membrane and GO/Nafion composite membrane (Z scale = 5°).

only exist in the part adjacent to the layer surface, just as demonstrated by the sectional SEM image of the GO deposit layer in Figure 1A2. Honestly, it is fairly difficult to exactly measure the GO content inside the Nafion matrix because of our distinctive preparation method. However, as the sectional SEM images of the proton exchange membranes shown in Figure 4C, D, the compatibility effect of GO on the two domains (hydrophobic backbone domains and hydrophilic ionic cluster domains) of Nafion matrix[20] is already evident. A typical diblock morphology is found in the recast Nafion membrane,[21] whereas it is thinner in the GO/Nafion composite membrane. This discovery is also confirmed by the XRD results (Figure 4E) that the peak intensity, proportional to the electron-density difference between the backbone domains and ionic cluster domains, is significantly weakened with GO being incorporated into the Nafion matrix.[20] Nanosized GOSs are embedded independently, tightly,[20,21] and randomly inside the membrane matrix, resulting from the independent-transfer property of GOSs, as indicated by sectional SEM and TEM images of the GO/Nafion composite membrane in images D and F in Figure 4 (and Figure S50 in the Supporting Information).

As illustrated by Figure 5A, B, both the humidity-dependent (80 °C) and temperature-dependent (40% RH) proton conductivity measurements demonstrate that the GO/Nafion composite membrane prepared by our method exhibits much higher proton conductivity than that of the recast Nafion membrane, especially under lower humidity. An increase in proton conductivity by several times could be easily observed in Figure 5A, B. Compared to the conductivity improvement of the proton exchange membranes prepared by simply adding (functionalized) GOSs into the polymer solution and then

sonicating the resultant mixture to help them disperse inside the polymer matrix, the conductivity enhancement observed here is much more prominent. Besides, as shown in Figure 5B, the recast Nafion membrane presents 78.14% decrased proton conductivity at 30 °C-40%RH compared with that under 90 °C-40%RH, whereas our GO/Nafion composite membrane possesses only 68.08% decreased proton conductivity at the same conditions, indicating that the stability of our GO/Nafion composite membrane is better. We believe that the increased water retention capability of the GO/Nafion composite membrane probably plays a positive part to some extent. Generally, any increase in WU leads to a certain increase in proton conductivity of the membrane.[21,23−26] The WU of the recast Nafion membrane is 20.51 wt %, which is comparable to that reported by others,[21,24] whereas the WU of GO/Nafion composite membrane slightly increases up to 22.38 wt %.

However, we doubt that such a slight improvement of the water retention capability could lead to such a great enhancement of proton conductivity. The rearrangement of backbones and ionic clusters attributable to the incorporation of GO probably has the major influence on the improvement of the proton conductivity. And this effect is considerable here (Figures 4E and 6), which could be ascribed to the good dispersion of these GOSs inside the Nafion matrix (Figure 4D, F). As the FT-IR spectra of the membranes illustrated in Figure 6A, the characteristic bands for $-CF_2-$ asymmetric and symmetric stretches could be found around 1212 and 1151 cm^{-1}, respectively.[20,21] Meanwhile, the band around 1055 cm^{-1} is attributed to the symmetric stretch of $-SO_3^-$.[20,21] Compared to the recast Nafion membrane, the broaden and/or shift of the former two bands of the GO/Nafion composite membrane demonstrates the existing of strong interactions of GOSs with the backbone domains of Nafion matrix, while the shift of the latter one illustrates the apparent influence of the incorporation of GOSs on the ionic cluster domains of Nafion matrix.[20,21] In addition, the strong interactions between the hydrophobic conjugation parts of GO and the backbone domains of Nafion matrix is also verified by the peak broadening and shifting in the XRD spectra, as shown in Figure 4E.[20] Figure 6C, D present the AFM images (phase images) of the recast Nafion and GO/Nafion composite membranes. Generally, the relatively lighter parts correspond to the softer hydrophilic ionic cluster domains, whereas the darker ones are assigned to the neutral hydrophobic backbone domains in the membrane.[27,28] Both the size and the connectivity of the ionic clusters are crucial to the membrane conductivity. The GO/Nafion composite membrane has relatively larger ionic clusters of varying sizes and better connectivity, which also positively affects the conductivity improvement of the composite membrane.[27] All the aforementioned facts intensively facilitate the proton transport in the case of GO/Nafion composite membrane, especially under low-humidity conditions (40% RH), as the activation energies calculated for both of the recast Nafion (22.82 kJ/mol, 40% RH) and GO/Nafion composite membrane (14.80 kJ/mol, 40% RH) in Figure 6B. Such a huge difference in activation energy explains well the result that the proton conductivity of the GO/Nafion composite membrane improves significantly. Besides, the rolled-up degree of the "evaporated" GOSs may be also crucial to the performance of the resultant proton exchange membranes, which is the major work of our further investigations.

4. CONCLUSIONS

Here, we successfully propose a facile approach to prepare rolled up GOSs with different topological structures via simply controlling the H_2O content in the original GOSs dispersion. Our method offers new degrees of freedom to investigate the transformation of those aforementioned allotropic forms of carbon and/or prepare some novel carbon/polymer composite materials. What's more, the formation of resultants (rolled up GOSs) is simultaneously accompanied by the separation of them from the reactants (the original GOSs dispersion), which is beyond the reach of other methods. Furthermore, it captures the gradual rolling process from GOSs into CNSs which agrees fairly with the long held notion that CNTs are rolled up graphene layers. Meanwhile, the porous (hole-like) graphene (oxide) material (indicated by Figure 3d, e) which has great potential applications in various fields[29−34] could be easily obtained by this way. The GO/Nafion composite membrane for proton exchange membrane fuel cell prepared based on such a porous GO material exhibits excellent proton conductivity. It is mainly attributed to the rearrangement of the microstructures of Nafion matrix by GOSs to significantly facilitate the proton transport. The method reported here will be of value to not only fundamental research but also industry because of its low energy cost, ability to be easily scaled-up, excellent repeatability, and simplicity.

■ ASSOCIATED CONTENT

Supporting Information

SEM images of the fresh aluminum foil surface (Figure S1); schematic illustration of the nomenclature applied in both the main text and the ESI (Figure S2); TG analyses of the fresh original aluminum foil and the sample "rolled up GO/aluminum foil" obtained at different H_2O contents (H_2O/DMF and H_2O/NMP) under 45 °C for 48 h (Figures S4/5); more TEM, SEM, and AFM characterizations of the rolled up GOSs prepared at 50/80 v/v% H_2O under 45 °C for 48 h (H_2O/THF) (Figures S6/7); Digital photos, AFM, surface, and sectional (FE-)SEM images of GO deposit layers on the aluminum surface under different evaporation conditions (H_2O/THF, H_2O/DMF, and H_2O/NMP) (Figures S3, S8−S49). Cross-sectional TEM images of the GO/Nafion composite membrane (Figure S50). This material is available free of charge via the Internet at http://pubs.acs.org.

■ AUTHOR INFORMATION

Corresponding Author

*E-mail: bbtang@fudan.edu.cn (B.T.); peiyiwu@fudan.edu.cn (P.W.). Tel.: +86-21-65643255. Fax: +86-21-65640293.

Notes

The authors declare no competing financial interest.

■ ACKNOWLEDGMENTS

The authors are very grateful for the financial support of the National Natural Science Foundation of China (NSFC) (21276051), Chinese doctoral fund (20110071130001), the Natural Science Foundation of Shanghai (12ZR1401900), and the National Basic Research Program of China (2009CB930000).

■ REFERENCES

(1) Geim, A. K.; Novoselov, K. S. *Nat. Mater.* **2007**, *6*, 183−191.

(2) Quintana, M.; Grzelczak, M.; Spyrou, K.; Calvaresi, M.; Bals, S.; Kooi, B.; Van Tendeloo, G.; Rudolf, P.; Zerbetto, F.; Prato, M. *J. Am. Chem. Soc.* **2012**, *134*, 13310−13315.
(3) Kosynkin, D. V.; Higginbotham, A. L.; Sinitskii, A.; Lomeda, J. R.; Dimiev, A.; Price, B. K.; Tour, J. M. *Nature* **2009**, *458*, 872−875.
(4) Zhang, Z. X.; Sun, Z. Z.; Yao, J.; Kosynkin, D. V.; Tour, J. M. *J. Am. Chem. Soc.* **2009**, *131*, 13460−13463.
(5) Wang, S.; Tang, L. A. L.; Bao, Q. L.; Lin, M.; Deng, S. Z.; Goh, B. M.; Loh, K. P. *J. Am. Chem. Soc.* **2009**, *131*, 16832−16837.
(6) Feng, K.; Cao, Y. W.; Wu, P. Y. *J. Mater. Chem.* **2012**, *22*, 11455−11457.
(7) Wang, X.; Yang, D.-P.; Huang, G.; Huang, P.; Shen, G.; Guo, S.; Mei, Y.; Cui, D. *J. Mater. Chem.* **2012**, *22*, 17441−17444.
(8) Savoskin, M. V.; Mochalin, V. N.; Yaroshenko, A. P.; Lazareva, N. I.; Konstantinova, T. E.; Barsukov, I. V.; Prokofiev, L. G. *Carbon* **2007**, *45*, 2797−2800.
(9) Yang, H. B.; Guai, G. H.; Guo, C. X.; Song, Q. L.; Jiang, S. P.; Wang, Y. L.; Zhang, W.; Li, C. M. *J. Phys. Chem. C* **2011**, *115*, 12209−12215.
(10) Li, Q.; Guo, B. D.; Yu, J. G.; Ran, J. R.; Zhang, B. H.; Yan, H. J.; Gong, J. R. *J. Am. Chem. Soc.* **2011**, *133*, 10878−10884.
(11) Wang, P.; Ao, Y.; Wang, C.; Hou, J.; Qian, J. *J. Hazard. Mater.* **2012**, *223*, 79−83.
(12) Yang, W. R.; Ratinac, K. R.; Ringer, S. P.; Thordarson, P.; Gooding, J. J.; Braet, F. *Angew. Chem., Int. Ed.* **2010**, *49*, 2114−2138.
(13) Zhu, Z.; Garcia-Gancedo, L.; Flewitt, A. J.; Xie, H.; Moussy, F.; Milne, W. I. *Sensors* **2012**, *12*, 5996−6022.
(14) Yang, X. Y.; Wang, Y. S.; Huang, X.; Ma, Y. F.; Huang, Y.; Yang, R. C.; Duan, H. Q.; Chen, Y. S. *J. Mater. Chem.* **2011**, *21*, 3448−3454.
(15) Yang, X. Y.; Zhang, X. Y.; Ma, Y. F.; Huang, Y.; Wang, Y. S.; Chen, Y. S. *J. Mater. Chem.* **2009**, *19*, 2710−2714.
(16) Viculis, L. M.; Mack, J. J.; Kaner, R. B. *Science* **2003**, *299*, 1361−1361.
(17) Kaempgen, M.; Lebert, M.; Haluska, M.; Nicoloso, N.; Roth, S. *Adv. Mater.* **2008**, *20*, 616−620.
(18) Shao, J. J.; Wu, S. D.; Zhang, S. B.; Lv, W.; Su, F. Y.; Yang, Q. H. *Chem. Commun.* **2011**, *47*, 5771−5773.
(19) Bai, H.; Li, C.; Wang, X. L.; Shi, G. Q. *J. Phys. Chem C* **2011**, *115*, 5545−5551.
(20) Choi, B. G.; Huh, Y. S.; Park, Y. C.; Jung, D. H.; Hong, W. H.; Park, H. *Carbon* **2012**, *50*, 5395−5402.
(21) Kumar, R.; Xu, C. X.; Scott, K. *Rsc Adv.* **2012**, *2*, 8777−8782.
(22) Shen, J. F.; Hu, Y. H.; Li, C.; Qin, C.; Ye, M. X. *Small* **2009**, *5*, 82−85.
(23) Xu, K.; Chanthad, C.; Gadinski, M. R.; Hickner, M. A.; Wang, Q. *ACS Appl. Mater. Interfaces* **2009**, *1*, 2573−2579.
(24) Zarrin, H.; Higgins, D.; Jun, Y.; Chen, Z. W.; Fowler, M. *J. Phys. Chem. C* **2011**, *115*, 20774−20781.
(25) Bae, B.; Miyatake, K.; Watanabe, M. *ACS Appl. Mater. Interfaces* **2009**, *1*, 1279−1286.
(26) Zhang, Z. H.; Wu, L.; Xu, T. W. *J. Mater. Chem.* **2012**, *22*, 13996−14000.
(27) Sekhon, S. S.; Park, J. S.; Cho, E.; Yoon, Y. G.; Kim, C. S.; Lee, W. Y. *Macromolecules* **2009**, *42*, 2054−2062.
(28) Affoune, A. M.; Yamada, A.; Umeda, M. *J. Power Sources* **2005**, *148*, 9−17.
(29) Huang, Z. H.; Liu, G.; Kang, F. *ACS Appl. Mater. Interfaces* **2012**, *4*, 4942−4947.
(30) Chen, Z. P.; Ren, W. C.; Gao, L. B.; Liu, B. L.; Pei, S. F.; Cheng, H. M. *Nat. Mater.* **2011**, *10*, 424−428.
(31) Yin, S. Y.; Zhang, Y. Y.; Kong, J. H.; Zou, C. J.; Li, C. M.; Lu, X. H.; Ma, J.; Boey, F. Y. C.; Chen, X. D. *Acs Nano* **2011**, *5*, 3831−3838.
(32) Gao, H.; Xiao, F.; Ching, C. B.; Duan, H. *ACS Appl. Mater. Interfaces* **2012**, *4*, 2801−2810.
(33) Xiao, J.; Mei, D. H.; Li, X. L.; Xu, W.; Wang, D. Y.; Graff, G. L.; Bennett, W. D.; Nie, Z. M.; Saraf, L. V.; Aksay, I. A.; et al. *Nano Lett.* **2011**, *11*, 5071−5078.
(34) Huang, X.; Qian, K.; Yang, J.; Zhang, J.; Li, L.; Yu, C.; Zhao, D. *Adv. Mater.* **2012**, *24*, 4419−4423.